# Inviscid double wake model for stalled airfoils



2014 J. Phys.: Conf. Ser. 524 012132

(http://iopscience.iop.org/1742-6596/524/1/012132)

# Inviscid double wake model for stalled airfoils

**L. Marion, N. Ramos-García[1], and J. N. Sørensen**
Department of Wind Energy, Fluid Mechanics Section, Building 403, Technical University of Denmark, DK-2800 Lyngby Denmark

E-mail: nerga@dtu.dk

**Abstract.** An inviscid double wake model based on a steady two-dimensional panel method has been developed to predict aerodynamic loads of wind turbine airfoils in the deep stall region. The separated flow is modelled using two constant vorticity sheets which are released at the trailing edge and at the separation point. A calibration of the code through comparison with experiments has been performed using one set of airfoils. A second set of airfoils has been used for the validation of the calibrated model. Predicted aerodynamic forces for a wide range of angles of attack (0 to 90 deg) are in overall good agreement with wind tunnel measurements.

## 1. Introduction

One of the main challenges in airfoil aerodynamics is to predict the airfoil characteristics at high angles of attack where most of the flow is separated. It is well-known that even Navier-Stokes solvers based on sophisticated turbulence modelling fail in predicting the correct behaviour at separation. A simple alternative, which has not been paid much attention, is to use a 2D panel method in which the separated region is modelled by vortex panels. This technique, which was originally proposed by Maskew and Dvorak [3] more than 35 years ago, has shown to be fast and produce relatively reliable results at massive separation. Inspired by their pioneering work, we have developed a so-called double wake model [5] which models the separated region.

The double wake model consists of a two-dimensional panel method in which a distribution of singularity elements is used to model both the airfoil geometry and the separated region. The model uses a surface distribution of constant sources and linear vortices along the airfoil geometry with a Neumann condition of no penetration as a boundary condition. The separation wake is represented by two constant vorticity sheets, released at the trailing edge and at the separation point, dividing the outer flow in two regions. In both regions the flow is considered as inviscid and irrotational. The double wake model is able to capture the correct pressure distribution over the airfoil once the separation location is known. Therefore the purpose of this study is to determine the correct wake length in function of the airfoil and the angle of attack and use it as an input to the solver in order to obtain the pressure distribution, the lift and the drag forces.

Thus, the aim of the present work is to predict stalled behaviour on airfoils in the region where CFD solvers show poor behaviour. The developed model has been implemented as a supplement to the Q$^3$UIC solver developed by Ramos-García et al. [1] at DTU Wind Energy. Merging these two

[1] To whom any correspondence should be addressed.

codes allows to simulate 0 to 90 degrees polar aerodynamic loads and provide good input to the Blade Element Momentum technique (BEM), which is the standard tool for design of wind turbines.

## 2. Numerical method and governing equations

### *2.1. Steady two-dimensional separated wake panel method*

A flow around a body $S_B$ having a free stream velocity $U_\infty$ is considered. For every point of a domain $V$ surrounding the solid body the velocity is defined as the sum of the free stream velocity and the induced velocity $u$

$$U = U_\infty + u \tag{1}$$

If the flow is considered to be incompressible, inviscid and irrotational, $u$ can be expressed as

$$u = -\nabla\Phi \tag{2}$$

where $\Phi$ is the potential satisfying the Laplace equation

$$\nabla^2\Phi = 0 \tag{3}$$

As the solid body surface $S_B$ is impermeable, the normal component of the velocity must be zero at the wall which gives a Neumann condition of no penetration across the body,

$$\nabla\Phi.n = 0 \tag{4}$$

The general solution to the Laplace equation is obtained through a source and vorticity distribution around the body contour. Hence the velocity induced by the solid body can be expressed as

$$u = u_\sigma + u_\gamma + u_{w1} + u_{w2} = -\nabla\Phi_\sigma - \nabla\Phi_\gamma - \nabla\Phi_{\gamma_{w1}} - \nabla\Phi_{\gamma_{w2}} \tag{5}$$

where $u_{w1}$ and $u_{w2}$ stand for the velocity induced by both vorticity sheets. The detailed expressions of the singularity elements potentials and their induced velocity have been implemented based on Katz & Plotkin [2].

The computed velocity at each panel center (collocation point) allows to calculate the pressure coefficient using the Bernoulli equation, [3]

$$Cp = 1 - \left(\frac{U}{U_\infty}\right)^2 + \frac{\Delta h}{\frac{1}{2}\rho {U_\infty}^2} \tag{6}$$

where $\Delta h$ stands for the increase in total pressure due to the suction of the separated region. The value of this head jump will be discussed and expressed in §2.3.

### *2.2. Double wake model*

The wake shape is obtained iteratively from an initial condition such as the one represented in Figure 1. Both vorticity sheets are represented as straight lines at the initial stage, which are connected downstream at a common point. After this initial stage they are shaped by the solver to follow the separated flow streamlines.

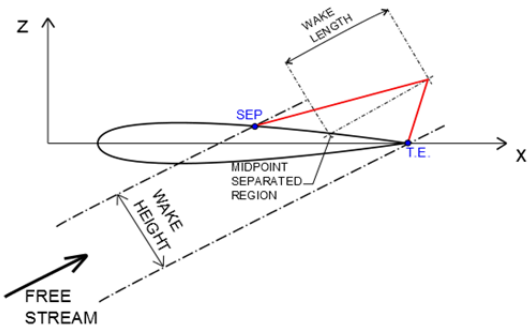


**Figure 1.** Airfoil and initial wake geometry.

The separation point in Figure 1 is represented somewhere on the suction side of the airfoil although this study is focused on the deep stall region where separation is assumed to take place at the leading edge. Under deep stall the separation location is no longer an unknown of the problem but a fixed parameter. Therefore the key parameter in this study is the wake length, $W_L$, defined as follows

$$W_L = W_F W_H \tag{7}$$

where $W_F$and $W_H$ stand for the wake factor and the wake height, respectively. $W_H$ is defined as the orthogonal distance between the stagnation point at the separation location (SEP) and the trailing edge (T.E.) at the initiation step (see Figure 1.). The $W_F$ parameter depends on the airfoil geometry and the angle of attack. More results concerning this factor are presented later on.

*2.3. Problem solving*

The total velocity potential is determined by the potential created by a linear distribution of vorticity and the one created by a constant source distribution. The wake is modeled by two free sheets represented by a number of panels with an uniform vorticity distribution. The strength of these two constant vorticity sheets is referred as $\gamma_{SEP}$ and $\gamma_{TE}$.

The potential model implemented consists of a linear distribution of vorticity, defining N+1 unknowns, one per panel edge ($\gamma_1..\gamma_{N+1}$). Here $\gamma_1$ is the trailing vorticity of the lower trailing edge panel and $\gamma_{N+1}$ represents the leading vorticity of the upper trailing edge panel. The strength of the two vorticity sheets $\gamma_{SEP}$ and $\gamma_{TE}$ are also unknowns. Therefore N+3 unknowns vorticity values ($\gamma_1..\gamma_{N+1},\gamma_{SEP},\gamma_{TE}$) have to be determined. To close the system of equations the following conditions are used:

- Neumann boundary condition of no penetration applied at each panel center (N equations)
- $\gamma_{TE} = \gamma_1$ as the vorticity sheet is leaving the airfoil from the trailing edge.
- Kutta condition: $\gamma_{SEP} = -\gamma_{TE}$
- Kutta condition consequence: $\gamma_{N+1} = 0$. All the vorticity arriving at the trailing edge is convected downstream to the wake sheet. For the same consideration, the vortex defined on the panel edge just after the separation point has no influence as the leading vortex of the “SEP” panel but only as the trailing vortex of the “SEP+1” panel (see Figure 2.).

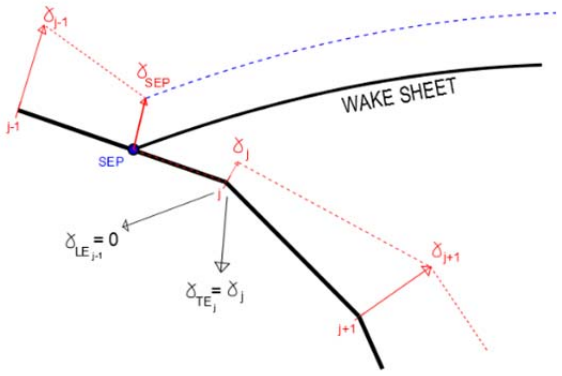


**Figure 2.** Close-up on the vorticty values around the separation location

Due to this set of conditions the system of equations is closed and the unknowns $(\gamma_1, \gamma_2, \dots, \gamma_{N+1}, \gamma_{TE}, \gamma_{SEP})$ can be determined.

As mentioned before the $C_P$ calculation is carried out using equation (6). As stated by Maskew and Dvorak [3], the head jump represents the increase in total pressure over that at infinity. Therefore $\Delta h = 0$ everywhere except over the separated region.

In the wake region, the head jump is expressed as the difference between the heads on both sides of the wake sheets. Considering the wake sheet shed from the separation point,

$$\Delta h = {h_{SEP}}^{-} - {h_{SEP}}^{+} \tag{9}$$

The steady Bernoulli equation is evaluated at the two sides of the SEP wake to obtain an expression for both heads and so on for the head jump

$$\Delta h = {h_{SEP}}^{-} - {h_{SEP}}^{+} = \left(\frac{U^2}{2}\right)_{SEP}^{-} - \left(\frac{U^2}{2}\right)_{SEP}^{+} \tag{10}$$

However, following Zanon et. al.[4], $\gamma_{SEP}$ can be expressed as

$$\gamma_{SEP} = {U_{SEP}}^{+} - {U_{SEP}}^{-} \tag{11}$$

and according to Voutsinas and Riziotis [5], all the vorticity is shed to the wake. It can then be assumed that the tangential velocity just under the wake sheet is zero e.g.

$${U_{SEP}}^{-} = 0 \tag{12}$$

which leads to

$$\Delta h = -\frac{{\gamma_{SEP}}^2}{2} \tag{13}$$

Therefore the pressure coefficient in the separated region is

$$Cp = 1 - \left(\frac{U}{U_\infty}\right)^2 - \frac{1}{\rho}\left(\frac{\gamma_{SEP}}{U_\infty}\right)^2 \tag{14}$$

## 3. Results

Computations of flows past different airfoils have been carried out using the numerical approach introduced above. A comparison with available experimental data from different wind tunnel tests is presented in order to validate the code and the assumptions made on the $W_F$.

A panel discretization of 170 for the airfoil and 25 for each vortex sheet has been used in all simulations. The airfoil has been discretized using a cosine distribution to provide a finer mesh at the leading and trailing edges.

### *3.1. Pressure distribution*

A validation of the code is hereby presented. The point of the validation is to ensure that the code is capable of capturing the characteristic pressure plateau of an airfoil under stalled conditions. In this section, the separation location is determined using the experimental data. A comparison with the results predicted by the *Q³UIC* code is presented herein to demonstrate the advantage of using the double wake model as an alternative to viscous-inviscid solvers in stalled regions.

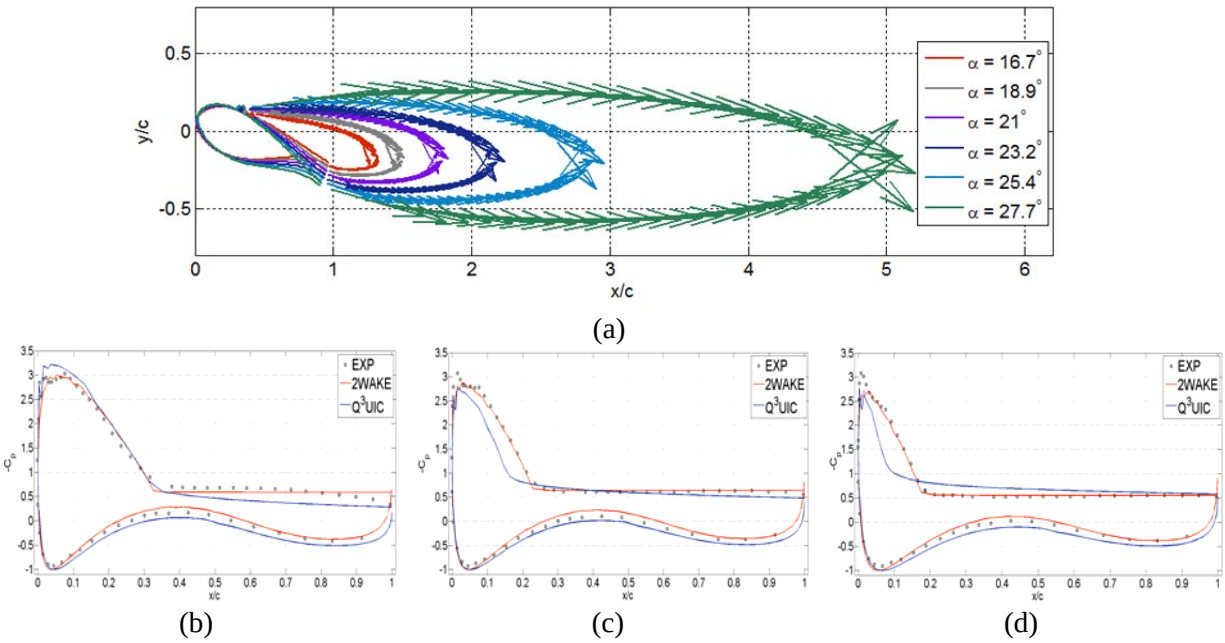


**Figure 3.** (a) Representation of the FFA-W3-301 airfoil and its converged wake shape at different angles of attack ; Pressure distribution around the airfoil in comparison to experimental data and Q³UIC at angles of attack (b) 16.7°, (c) 21° and (d) 27.4°.

Measurements of the flow past the FFA W3 301 (30% thickness) airfoil were performed at Risø National Laboratory in the VELUX wind tunnel at a Reynolds number of $Re = 1.6e^6$ and collected in Fulgsang et. al. [6]. The viscous-inviscid simulations have been performed with the Q³UIC solver using a 140 panels surface mesh, free laminar to turbulent transition and a turbulence intensity of 0.1%. In the double wake simulations the computed pressure distribution has been obtained fixing the separation location at $x/c = \{0.35; 0.25; 0.19\}$ at angles of attack $\alpha = \{16.7; 21; 27.4\}$ deg respectively. The optimum $W_F$ is obtained through comparison with the measured pressure distribution. The obtained wake factors were $W_F = \{1.6; 2.4; 3.9\}$ resperctively, with subsequent wake lengths $W_L/c = \{0.53; 0.99; 1.88\}$.

An excellent overall agreement with experiments on both pressure and suction side is obtained, capturing the correct pressure level in the separated region. In comparison with Q³UIC simulations, the double wake model predicts more accurately the suction peak as well as the pressure level in the

separated region. The wake length is increasing with the angle of attack and appears as a key variable for the accuracy of the predictions.

*3.2. Wake factor*

The present work is focused on the deep stall region, meaning that the separation location is at the leading edge. With the separation location prescribed, $W_F$ is the key parameter in the simulations. Therefore the evolution of $W_F$ as a function of the angle of attack for different airfoil geometries has been studied.

The following airfoils for which experimental data at high angles of attack is available have been used [7] [8] [9] [10] [11] [12]. The study is based on the comparison between the computed lift coefficient, $C_l$, obtained by integrating the pressure distribution, and the experimental $C_l$. In Figure 4 the eight airfoils used for the study are represented. Six airfoils have been used to determine the $W_F$ trend law as a function of the angle of attack. The remaining ones have been kept apart in order to validate the computed trend law.

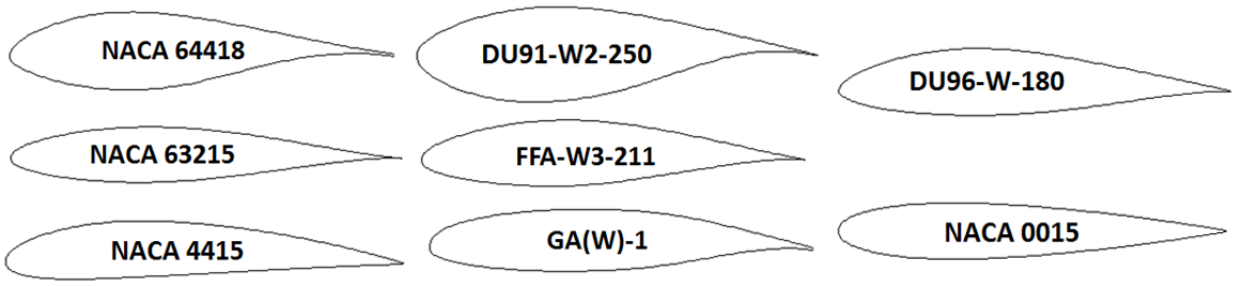


**Figure 4.** Contours of the 8 airfoils used for the $W_F$ study: (a) airfoils used to determine the $W_F$ trend law and (b) airfoils used to validate the trend law.

For the six airfoils used as benchmark, simulations have been run forcing the separation at the L.E., while finding the optimum $W_F$ in the range [1: 40]. For each angle of attack the optimum $W_F$ is obtained through comparison with the experimental $C_l$.

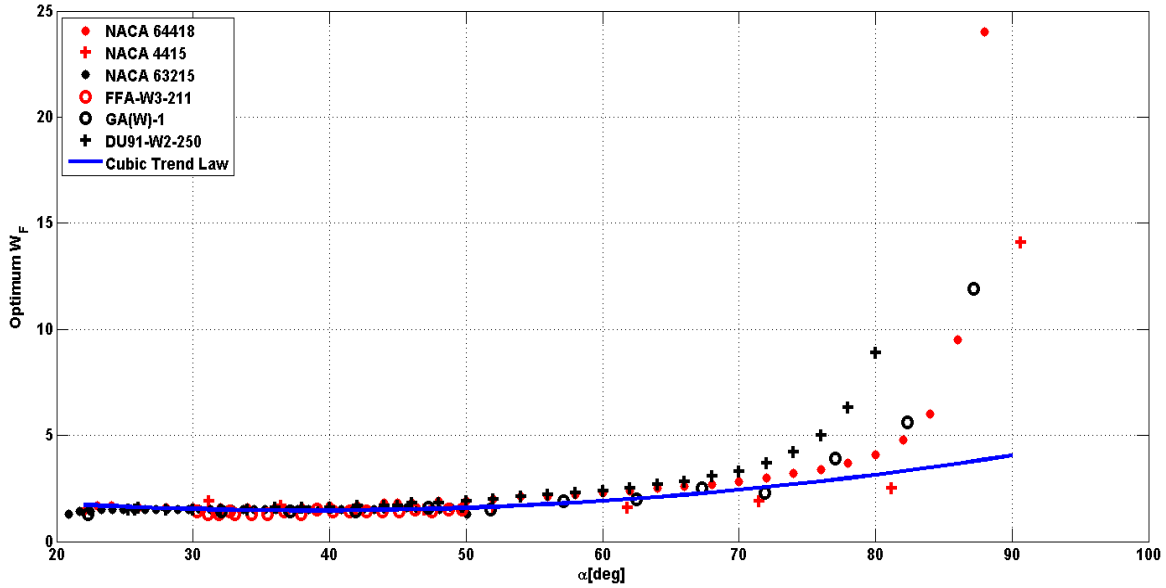


**Figure 5.** Optimum $W_F$ obtained through $C_L$ comparison for six airfoils in function of the angle of attack

At angles of attack lower than 50 deg all airfoils give similar optimum $W_F$ with values in the vicinity of $W_F = 1.5$. A quadratic trend law has been extracted for every airfoil within the range $\alpha = [20; 60]$ and the results extrapolated to all inflow angles. An average trend law has been calculated expressing the $W_F$ with the following coefficients (see Figure 5.)

$$W_F = 9.8.10^{-4}\alpha^2 - 7.5.10^{-2}\alpha + 2.9 \quad (15)$$

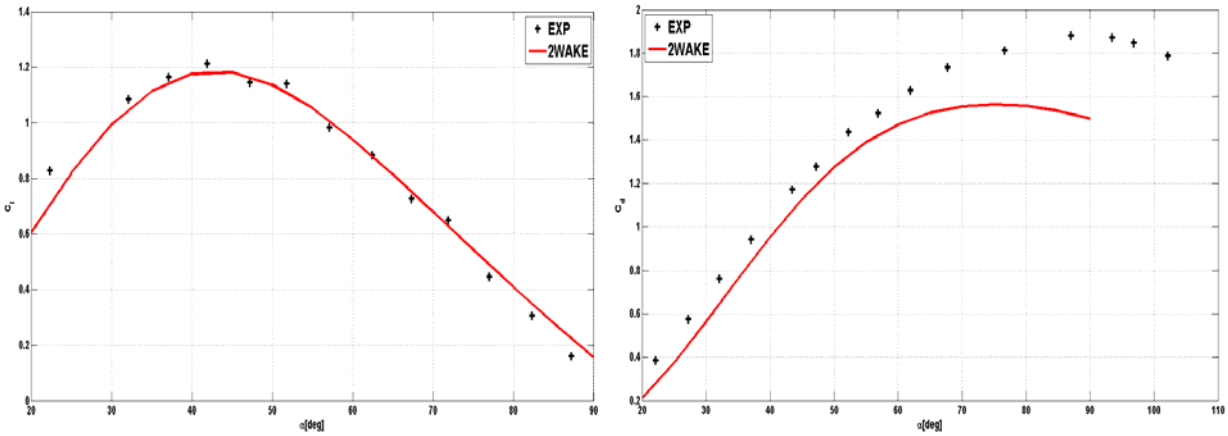


(a) (b)

**Figure 6.** Comparison between experimental and double wake simulations for flows past the GA(W)-1 at $R_e = 0.67e6$ (a) $C_l$, (b) $C_d$

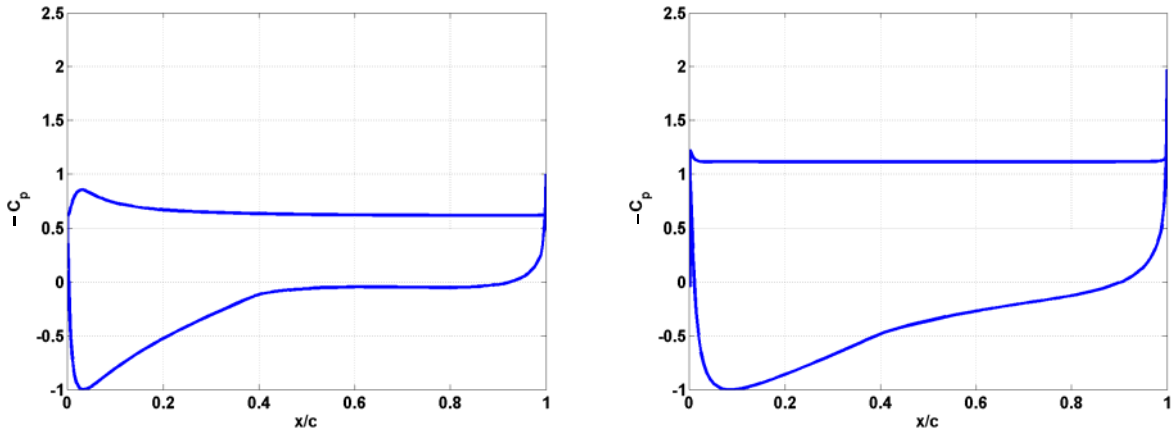


(a) (b)

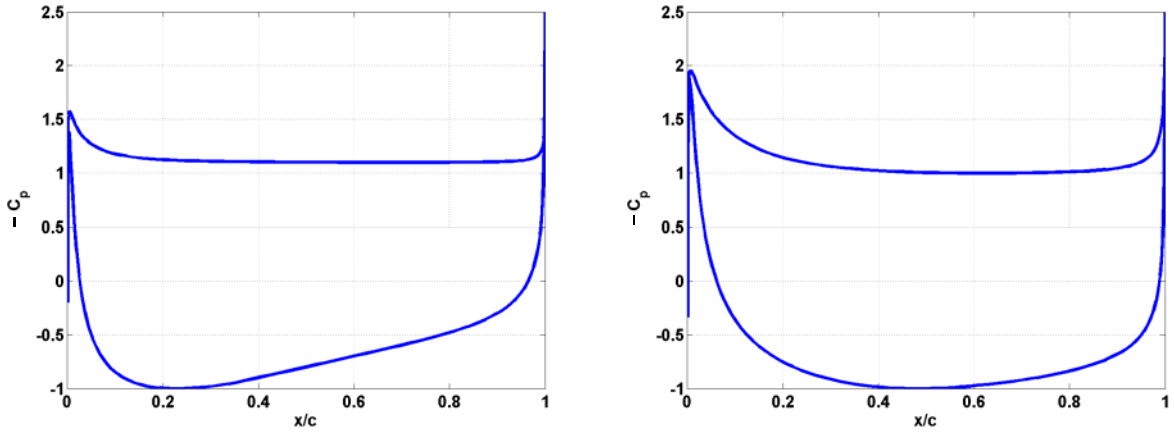


(c) (d)

**Figure 7.** Predicted pressure distributions for flow past the NACA 64418 airfoil at angles of attack (a) 23 (b) 41 (c) 65 and (d) 90 deg.

As seen in Figure 6(a), the re-computation of $C_l$ with the $W_F$ obtained from the trend law is in good agreement with the experimental data. It appeared that the $C_l$ calculation is more sensitive to $W_F$ in the lower angle of attack range ($\alpha < 60°$) than in the higher range ($60° < \alpha < 90°$). However the re-computation of the $C_d$ shows not such a good agreement at high angles of attack. The optimum $W_F$ study has been done through $C_l$ comparison which could explain discrepancies on the $C_d$. The $C_d$ is calculated taking only into account the pressure drag. At such high angles of attack we can neglect the viscous drag.

The model predictions of the surface pressure coefficient are plotted in Figure 7. It can be appreciated that, as expected, the suction side plateau remains at the same value while on the pressure side the stagnation point is moving downstream and is located at $x/c = 0.5$ at $\alpha = 90°$.

### *3.3. Merging with Q³UIC – full polar aerodynamic loads*

The trend law obtained for the $W_F$ parameter is now used to predict the aerodynamic loads for the two airfoils used for the calibration of the model. The predicted results are compared with the experimental data in what follows. The double wake computations are merged with the Q³UIC computations which are carried out at the low angles of attack region. In this way the full polar is obtained over the full $\alpha = [0; 90]$ range.

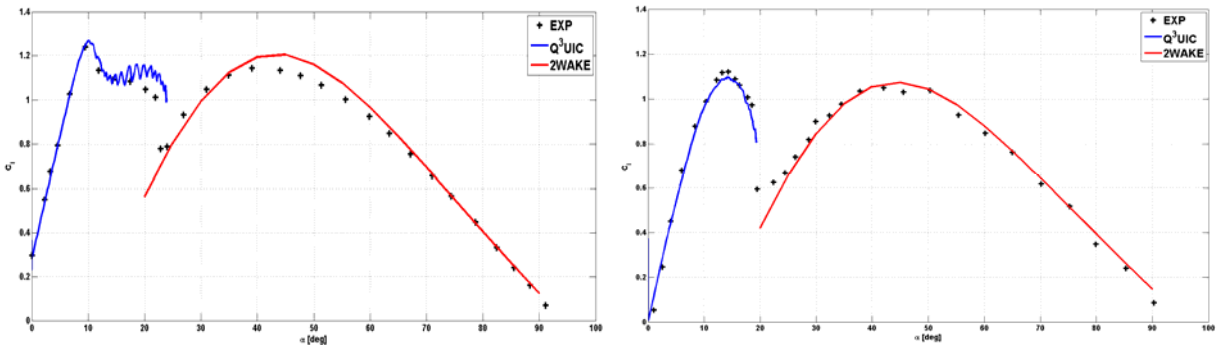


(a) (b)

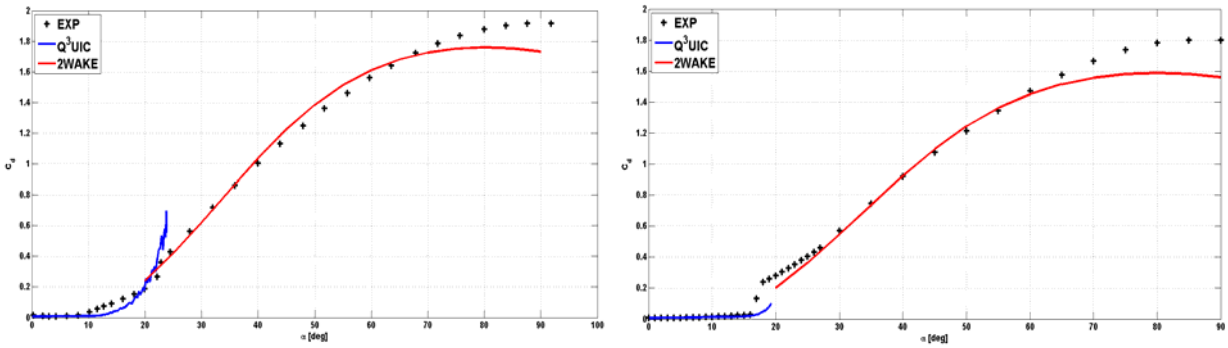


(c) (d)

**Figure 8.** Comparison between experimental and computed $C_l$ (upper) and $C_d$ (lower) curves at $Re = 0.7e6$ for (a),(c)DU96-W-180, (b)(d) NACA 0015.

Both codes are aimed at being combined in the future, with the double wake model performing computations at massive separation and employing the Q$^3$UIC code at attached and mildly separated flows.

As seen in Figure 8, the re-computation of $C_l$ and $C_d$ with the $W_F$ obtained from the trend law is in good agreement with the experimental data. On both $C_l$ and $C_d$ curves the difference between computed and experimental data never exceeds 10%. On Figure 8(c) Q$^3$UIC code over-predicts the $C_d$ values just before it fails converging due to the large amount of separated flow. When the separation location is getting to close to the L.E. (within the 10 first percent of the chord) the code doesn't manage to capture the suction peak reduction.

## 4. Conclusion

To predict airfoil characteristics for massively separated airfoils, a double wake model has been developed and validated against different experimental data in the deep stall range. The wake factor $\boldsymbol{W_F}$ variation against the angle of attack has been modeled by a cubic trend law, based on a study carried out with six airfoils benchmark. The model generally predicts airfoil characteristics in very good agreement with experimental data, provided that the separation point is located close to the leading edge. Some discrepancies appear around the deep stall $\boldsymbol{C_{l\,max}}$ and $\boldsymbol{C_{d\,max}}$. In this region the code is under-predicting the aerodynamic loads. A future use of the code is to combine it with the Q$^3$UIC code in order to predict full airfoil polar. Another use of the code will be to employ it to simulate thick airfoils where the point of separation is mainly determined by the geometry.

## 5. Acknowledgments

The present work has been carried out with the support of the Danish Council for Strategic Research for the project 'Center for Computational Wind Turbine Aerodynamics and Atmospheric Turbulence' (grant 2104-09-067216/DSF) (COMWIND) (http://www.comwind.org).
The authors would like to acknowledge Anders Björck and the Aeronautical Research Institute of Sweden for their cooperation in providing experimental data.

## References

[1] N. Ramos-García, J.N. Sørensen and W.Z. Shen 2013, *Three-Dimensional Viscous-Inviscid Coupling method for Wind turbine Computations.* Submitted to Wind Energy.
[2] J. Katz and A. Plotkin 1977, Low speed aerodynamics: from wing theory to panel methods *McGraw-Hill*
[3] B. Maskew and F.A. Dvorak 1978, The Prediction of $\boldsymbol{C_{l\,max}}$ Using a Separated Flow Model. *Journal of the American Helicopter Society*
[4] A. Zanon, P. Giannattasio and C.J. Simão Ferreira 2012, A vortex panel method for the simulation of the wake flow past a vertical axis wind turbine in dynamic stall. Published online in Wind Energy

[5] V.A. Riziotis, S.G. Voutsinas 2008, Dynamic stall modelling on airfoils based on strong viscous inviscid interaction coupling. *International Journal for Numerical Methods in Fluids*; 56: 185–208. DOI: 10.1002/fld.1525.
[6] P. Fuglsang, I. Antoniou, K.S. Dahl and H. Aagaard Madsen 1998, *Wind tunnel tests of the FFA-W3-241, FFA-W3-301 and NACA 63-430 airfoils*. Denmark. Forskningscenter Risø. Risø-R, no. 1041(EN)
[7] W.A. Timmer and R.P.J.O.M. van Rooij 2001, Some aspects of high angle-of-attack flow on airfoils for wind turbine application. *Proceedings of the European wind energy conference.*
[8] A. Björck, Wind tunnel test of FFA-W3-211 and NACA 63-215. Flygtekniska Försöksanstalten. Personal communication.
[9] J.G. Schepers and K. Boorsma 2009, Description of experimental setup MEXICO measurements. *Final report of IEA Task 29, Mexnext (Phase 1).*
[10] W.A. Timmer 2010, Aerodynamics characteristics of wind turbine blade airfoils at high angles-of-attack. *Journal of Physics: Conference series, The Science of Making Torque from Wind.*
[11] C. Ostowari and D. Naik 1985, Post-Stall Wind Tunnel; Data for NACA 44XX; Series Airfoil Sections. SERI Technical Monitor, SERI Task N. 4807.20; FTP N. 495, US Department of Energy, Contract N. DE.AC02.83CH10093.
[12] R.E. Sheldahl, P.C. Klimas 1981, Aerodynamic Characteristics of Seven Symmetrical Airfoil Section Through 180-Degree Angle of Attack for Use in Aerodynamic Analysis of Vertical Axis Wind Turbine. *Report SAND80-2114, Sandia Laboratories, Albuquerque.*